CEBAF PROPOSAL COVER SHEET

This Proposal must be mailed to:

CEBAF
Scientific Director's Office
12000 Jefferson Avenue
Newport News, VA 23606

and received on or before 1 October 1991.

A. TITLE: MEASUREMENT OF THE DIFFERENTIAL CROSSECTIONS FOR $p(\gamma,K^+)\Lambda$ AND $p(\gamma,K^+)\Sigma^0$ AT $\theta_{CM}=90°$ AND $1.4 \leq E_\gamma \leq 3.4$ GeV

B. CONTACT PERSON: J. NAPOLITANO

ADDRESS, PHONE, AND ELECTRONIC MAIL ADDRESS:

PHYSICS DIVISION, MAIL STOP 12H
CEBAF
JIMNAP@CEBAF

C. IS THIS PROPOSAL BASED ON A PREVIOUSLY SUBMITTED PROPOSAL OR LETTER OF INTENT?

[ ] YES [X] NO

IF YES, TITLE OF PREVIOUSLY SUBMITTED PROPOSAL OR LETTER OF INTENT

****

(CEBAF USE ONLY)

Receipt Date 20 SEP 91

Log Number Assigned PR 91-001

By [redacted]

CEBAF Proposal to PAC5: Measurement of the Differential Cross Sections for $p(\gamma, K^+)\Lambda$ and $p(\gamma, K^+)\Sigma^0$ at $\theta_{CM} = 90°$ and $1.4 \leq E_\gamma \leq 3.4\ GeV$

J.Napolitano (Spokesperson), O.K.Baker, R.Carlini
Y.Chen, D.Mack, W.Vulcan, S.Wood
Physics Division, CEBAF

S.Bart, R.E.Chrien, R.Sawafta, R.J.Sutter
Physics Department, Brookhaven National Laboratory

E.J.Beise, B.W.Filippone, W.B.Lorenzon, R.D.McKeown
Kellogg Radiation Laboratory, Caltech

E.Kinney, R.J.Peterson, R.Ristinen
Physics Department, University of Colorado

E.V.Hungerford, K.Lan, B.W.Mayes, L.G.Tang
Physics Department, University of Houston

A.Klein
Physics Department, Old Dominion University

R.Gilman
Physics Department, Rutgers University

September 20, 1991

Abstract

We propose to measure two-body photoproduction of K^+ from the proton, leading to $K^+\Lambda$ and $K^+\Sigma^0$ final states, for $\theta_{CM} = 90°$ and for photon energies between 1.4 and 3.4 GeV. No measurements have been made between 1.7 and 4 GeV. Existing data is qualitatively different at low and high energies and it has been suggested that quarklike degrees of freedom are relevant for $E_\gamma \geq 4$ GeV. The experiment can be done using equipment already needed for approved experiments in Hall C, and makes little demand on the accelerator.

1 Introduction

The dynamics of strange quarks and their relation to nucleon structure is a much discussed subject in strong interaction physics. For example, "hidden strangeness" in the nucleon has been suggested experimentally. That is, even though the nucleon has no net strangeness, dynamics of the $s\bar{s}$ sea may account for some of the nucleon's mass, spin, magnetic moment, and charge radius [1]. It may be possible to gain a handle on understanding these effects by studying processes where strangeness is directly produced. For example, some fraction of the time the nucleon may be a strange baryon with a strange meson "cloud" and the experimental meson-nucleon-baryon couplings are used to predict various "hidden strangeness" matrix elements [2]. Direct strangeness production gives us these couplings.

Exclusive K^+ photoproduction from the proton is a primary source of information on strange meson-baryon-nucleon interations. Various analyses [3, 4, 5, 6] use this data to extract the various couplings in the context of "effective field theories" [5]. For example, two recent works [5, 6] analyze data on $\gamma p \rightarrow K^+\Lambda$ for $E_\gamma \leq 1.4$ GeV in terms of energy-independent coupling constants and obtain reasonably good fits. There is little data above 1.4 GeV.

An entirely different picture of $\gamma p \rightarrow K^+\Lambda$ and $\gamma p \rightarrow K^+\Sigma^0$ is based on the notion that hadrons are composed of "pointlike constituents", e.g. quarks. The "constituent counting rules" [7, 8] state that for any exclusive reaction $A + B \rightarrow C + D$, the differential cross section $d\sigma/dt \rightarrow f(\theta_{CM})/s^{n-2}$ (as s, t, and $u \rightarrow \infty$), where n is the total number of pointlike constituents. Some data above 4 GeV suggest that $d\sigma/dt \propto 1/s^7$ for K^+ photoproduction, but the evidence is not strong. In addition, such behavior would be poorly understood if we assume that the constituents are quarks and their interactions are governed by QCD [9, 10].

Almost no data on the differential cross sections exists between $\approx$ 1.5 and 4 GeV. See Fig. 1. We propose to begin to fill in the gap by measuring at $\theta_{CM} = 90°$ for $1.4 \leq E_\gamma \leq 3.4$ GeV. Existing data suggest that $\theta_{CM} = 90°$ may be a good place to look first for signs of a $1/s^7$ dependence. The limits on E_γ are imposed for technical reasons.

Measurements will be done with a bremsstrahlung endpoint technique, using a thin upstream radiator and with the electron beam passing through the liquid hydrogen target. We will detect the K^+ in singles using the SOS spectrometer in Hall C. Rate from virtual and real photoproduction via electron beam interactions in the target will be subtracted by removing the radiator. This technique was successfully used in a measurement, largely by members of the same collaboration, of high energy deuteron photodisintegration [11]. The momentum and angle acceptance of the SOS allows both $K\Lambda$ and $K\Sigma$ final states to be measured simultaneously for a given beam energy and spectrometer settings so no cross calibrations are necessary. The momentum resolution allows a large range of photon energies between the $K\Lambda$ and $K\Sigma$ thresholds, and between the $K\Sigma$ and $K\Lambda\pi^0$ (i.e. background) thresholds. The $K\Sigma$ cross section will be extracted by subtracting the $K\Lambda$ cross sections measured in this same experiment. If need be, the SOS can be left at a fixed angle of 39°. Particle identification will be done with equipment already under construction for the SOS, namely Time-of-Flight (TOF) hodoscopes and an aerogel Cerenkov counter. Detected K^+ rates are on the order of $1/sec$ at the highest energies, using modest beam current and target.

We emphasize that this proposal is quite complementary to proposal PR-89-004 [12] which will measure these reactions using the CLAS. That group will simultaneously measure the cross section for energies up to 1.8 GeV or so, and a wide range of center of mass angles. Their aim is to help determine strange hadron couplings in an energy regime where that formulation should be reliable. Our proposal concentrates on high energy and momentum transfer by bridging the large gap between the existing data, trying to identify energies at which the $1/s^7$ behavior commences. Figure 1 shows, on a plot of θ_{CM} versus E_γ, where data currently exists as well as the regions covered by the two experiments.

2 Physics Motivation

Phenomenological $KN\Lambda$ and $KN\Sigma$ couplings have been determined with some success by several investigators [3, 4, 5, 6]. These analyses use a large body of data on the reactions $\gamma p \rightarrow K^+\Lambda$ ($E_{thresh} = 0.911\ GeV$) and $\gamma p \rightarrow K^+\Sigma^0$ ($E_{thresh} = 1.046\ GeV$) acquired through the early 1970's [13]–[25], using photon energies up to $\approx 1.7\ GeV$. The analyses are quite model dependent, given the various poles and associated couplings that might be involved [5]. In fact, a resonance with mass $\approx 1.9\ GeV$ coupling to $K\Sigma$ is suggested on the basis of the behavior of the $\gamma p \rightarrow K^+\Sigma^0$ cross section near $E_\gamma = 1.4\ GeV$ [23].

All in all, these effective field theory models do a generally good job describing the cross section at low energies. This is despite the fact that the coupling constants are independent of energy and momentum transfer. Figure 2, reproduced from Ref. [5], shows the data for $\gamma p \rightarrow K^+\Lambda$ at $E_\gamma = 1.3\ GeV$ compared to various models. Data at $\theta_{CM} \leq 90°$ [20, 21, 23] are shown, but data also exist at backward angles [24]. Free parameters are determined by fitting to the body of differential cross section data (for $E_\gamma \leq 1.4\ GeV$), to available

Λ recoil polarization data, and to the measured $p(K^-,\gamma)\Lambda$ capture rate using a crossing-consistent analysis. The agreement is quite satisfactory. A CEBAF experiment using the CLAS [12] will provide a large body of data in this energy region which should help better determine the free parameters.

There exists a bit more data on these reactions, however, in a very different regime, namely at high photon energy and momentum transfer [26]. In that experiment, cross sections for reactions of the sort $\gamma p \to meson + baryon$ were studied for photon energies above 4 GeV and at center of mass angles near 90° where the momentum transfers t and u to both final state particles is large. The general conclusion was that the cross sections followed the "constituent counting rules" [7, 8] which assume that the hadrons are composed of pointlike particles, and that the interactions between these particles are not strong. In particular, the cross section $d\sigma/dt$ should behave like $f(\theta_{CM})/s^7$, $s \equiv E_{CM}^2$, where the power of s is gotten by subtracting 2 from the number of "fundamental fields" in the reaction. The normalization function $f(\theta_{CM})$ is not specified, but can in principle be calculated assuming that perturbative QCD correctly describes this behavior [10].

If one accepts the evidence that $d\sigma/dt \propto 1/s^7$ for meson photoproduction at high energies, then the reason for this behavior is not well understood and would actually be quite surprising. For example, the observed magnitude of the cross section is inconsistent with the assumption that only the minimal number of quarklike degrees of freedom are important [9]. In fact, existing perturbative QCD calculations [10] give only moderate agreement with the data. The calculations differ most strongly for θ_{CM} larger than about 60°, and the authors suggest that $u-$channel baryonic resonances need to be taken into account. For $K\Lambda$ and $K\Sigma$ photoproduction, the calculated cross sections are too small by roughly an order of magnitude.

The bulk of the data taken at high energy and momentum transfer is for $\pi^\pm$ and π^0 production, and the strongest conclusions of Ref. [26] are based on that data. However, let us now consider the K^+ data. In Fig. 3 we reproduce the data of Ref.[26] which shows $s^7 d\sigma/dt$ for $K\Lambda$ and $K\Sigma$ photoproduction, plotted as a function of $\cos\theta_{CM}$. The data, measured only at 4 and 6 GeV, suggest the simple $1/s^7$ behavior is relevant, although the statistical variations are quite large. (Note that the cross sections $d\sigma/dt$ differ by more than an order of magnitude.) This appears to be true over the whole angular range. The lines through the points are empirical fits to the functional form $(1-z)^{-5}(1+z)^{-4}$, $z \equiv \cos\theta_{CM}$. This form seems to describe the high energy cross sections for $\gamma p \to \pi^+ n$ over the entire angular range [26]. We use this form here to characterize the shape of the $K\Lambda$ and $K\Sigma$ data.

How are we to reconcile empirical descriptions based on effective coupling constants [3, 4, 5, 6] in the face of this surprising and poorly understood behavior at high energy [8, 9, 10]? Figure 4 plots the cross section for $\gamma p \to K^+\Lambda$ at $E_\gamma = 1.3\ GeV$, scaled by s^7 as in Fig. 3. (This is the same data plotted in Fig. 2, plus the data at $\theta_{CM} > 90°$.) It is at least clear that some qualitative difference takes place between low and high en-

ergies. More data in the intermediate energy region is necessary to try to disentangle the descriptions.

We focus our attention on the region near $\theta_{CM} = 90°$ where all the momentum transfers are comparable. Figure 5 shows measured cross sections for both $K\Lambda$ and $K\Sigma$ photoproduction near $\theta_{CM} = 90°$. Notice that the cross section changes by nearly three orders of magnitude. The highest energy data other than that taken at SLAC [26] ($E_\gamma = 4$ and 6 GeV) is from DESY [23] and extends up to around 1.7 GeV. Figure 5 also plots a model calculation of the cross section at low energies [4] (solid line), completed before the DESY data became available. We would like to compare the data to $d\sigma/dt = constant/s^7$, but we must choose some normalization. Figure 5 also shows this prediction normalized to the data point at 4 GeV (dashed line) and to the empirical fit shown in Fig. 3 (dotted line). All the predictions vary significantly, but there is a suggestion that a scale based on s^7 is an appropriate bridge between the two energy regions. On the other hand, the perturbative QCD calculations [10] suggest that baryonic resonances might be important here, and both Λ and Σ resonances with masses between 1.8 and 2.2 GeV (corresponding to photon energies between 1.3 and 2.1 GeV) have been observed [27] which decay to $N\bar{K}$. The suggestion [23] that the $\gamma p \rightarrow K^+\Sigma^0$ data shows a resonance with mass ≈ 1.9 GeV ($E_\gamma \approx 1.4$ GeV), for example, can only be tested by acquiring data into the region past $E_\gamma = 2$ GeV (Fig. 5).

The behavior of the cross sections in the intermediate energy range between ≈ 1.5 and 4 GeV is clearly crucial to our understanding of these processes. **We propose to measure these cross sections at $\theta_{CM} = 90°$ between $E_\gamma = 1.4$ GeV, where there is significant overlap with previous experiments, and $E_\gamma = 3.4$ GeV which nearly closes the gap with the SLAC results [26].** This would be the first step in determining the behavior in this region. We are strongly interested in making subsequent measurements at other angles, but this first experiment makes minimal demand on the accelerator and spectrometer soon after CEBAF startup. Possible extensions to this work are outlined at the end of this proposal.

3 Experimental Technique

We will measure the reactions $p(\gamma, K^+)\Lambda$ and $p(\gamma, K^+)\Sigma^0$ at $\theta_{CM} = 90°$ for photon energies from 1.4 GeV up to 3.4 GeV. Untagged bremsstrahlung near the kinematic endpoint will be used as a photon source, and the SOS spectrometer in Hall C will detect the K^+ in singles. $E_\gamma \geq 1.4$ GeV is dictated by the desire to include both $K\Lambda$ and $K\Sigma$ final states into the SOS acceptance, and to minimize K^+ decay losses. The high energy photon limit (3.4 GeV) is imposed by the maximum central momentum of the SOS (1.8 GeV/c). The layout is shown schematically in Fig. 6a. The bremsstrahlung radiator is located approximately 1 m upstream of the liquid hydrogen target, and so both photons and electrons pass through the target on the way to the beam dump. K^+ produced directly by interactions of the electron beam in the target are subtracted by taking data with the radiator removed.

Because of limited resolution and reconstruction capability, most previous experiments (for example, Ref. [23]) measured the K^+ yield integrated over large portions of the spectrometer acceptance as a function of incident beam energy for fixed K^+ momentum. On the other hand, if the K^+ are analyzed with a large enough momentum bite and fine enough resolution, the beam energy is kept constant and the K^+ momentum spectrum shows the onset of the $K\Lambda$ and $K\Sigma^0$ final states. Figure 6b shows data taken in this way using the SLAC 1.6 GeV spectrometer [28]. Given the calculated bremsstrahlung spectrum [29], it is straightforward to determine the cross section for $p(\gamma, K^+)\Lambda$ up to the $p(\gamma, K^+)\Sigma^0$ threshold, and the $p(\gamma, K^+)\Sigma^0$ cross section up to the $p(\gamma, K^+)\Lambda\pi^0$ threshold. A similar technique has been u sed to measure deuteron photodisintegration also using the SLAC 1.6 GeV spectrometer [11].

The SOS spectrometer [30] is nearly ideal for our kinematics. Firstly, its intent is to provide a means to momentum analyze unstable particles by virtue of its short optical length. For the lowest momenta we consider, the survival fraction of K^+ is in excess of 10%. Second, its large in-plane angular acceptance (± 60 mr) makes it possible to access a large range of center of mass angles simultaneously. This will allow us to interpolate precisely to $\theta_{CM} = 90°$. Third, its large solid angle ≈ 7.5 msr insures a reasonable rate even at high energy where the cross section may be quite small[1].

Lastly, the SOS has a very large momentum bite ($\pm 20\%$) making it possible to include both $K\Lambda$ and $K\Sigma$ final states for E_γ as low as 1.4 GeV. Figure 7 shows the loci of thresholds for $K\Lambda$, $K\Sigma$, and $K\Lambda\pi^0$ final states, plotted as a function of K^+ laboratory momentum versus angle, for beam energies of 1.4 GeV and 3.4 GeV, and for θ_{CM} near 90°. The limits on the plots are given by the SOS momentum and angle acceptances. Hence, for a single incident electron beam energy, we can determine the cross sections over a substantial part of the photon spectrum.

[1] An alternative tune of the SOS, based on parallel-to-point transverse optics, rather than point-to-point, is being investigated. We would gain angular resolution at the expense of in-plane angle acceptance and so solid angle, although longer targets would be allowed.

3.1 $p(\gamma, K^+)\Lambda$ and $p(\gamma, K^+)\Sigma^0$ Kinematics and Rates

We calculate rates using the $p(\gamma, K^+)\Lambda$ cross section scaled by s^7 from 4 GeV. (The $K\Lambda$ and $K\Sigma$ cross sections appear to be very comparable to each other over all energies.) We assume the following beam, target, and spectrometer parameters:

- Beam current is $10\mu A$
- LH2 Target length is 4 cm
- Radiator thickness is 6% R.L.
- Spectrometer solid angle is 7.5 msr
- Photon energies at least 20 MeV below endpoint
- K^+ must travel at least 10 m to be identified.

The beam current is modest and the (electron beam) luminosity is around $10^{37}/cm^2sec$, well within the expected tolerance of the SOS [30]. The power absorption in the target is $\approx 12\ W$, and relatively simple targets have been built which would suffice [31]. A 6% radiator has been successfully used in a previous photoproduction experiment [11].

Table 1 lists relevant kinematics and rates using the above assumptions. The difference between momenta for the $K\Lambda$, $K\Sigma$, and $K\Lambda\pi^0$ thresholds is small enough at $E_\gamma = 1.4\ GeV$ so that the reactions of interest are fully contained in the $\pm 20\%$ momentum bite. The difference is large enough at $E_\gamma = 3.4\ GeV$ so that the spectrum can be binned relatively finely given the $\approx 10^{-3}$ momentum resolution. The photon energy bite between the bremsstrahlung endpoint steps is around 100 MeV. The decay length λ is such that losses are always less than 90%. Note that the laboratory angle corresponding to $\theta_{CM} = 90°$ does not vary much. The momentum dependence on angle is not strong (see Fig. 7), so only modest angular resolution is required.

3.2 Background Rates

There are three general kinds of background to consider. One is the rate of K^+ from reactions in materials other than hydrogen, presumably the target windows. Second and third are the rates of protons and pions from reactions in hydrogen and in the target windows. A distinctive feature of $K\Lambda$ and $K\Sigma$ photoproduction is the bremsstrahlung step (see Fig. 6) and so all backgrounds are "kinematically distinct" at some level. Protons and pions will be directly eliminated by particle identification. (We discuss the particle identification requirements in Section 4.)

Table 1: Kinematics and Rates for $p(\gamma, K^+)(\Lambda, \Sigma)$ at $\theta_{CM} = 90°$. We include the momentum bites $\Delta p/p$ corresponding to the difference in bremsstrahlung endpoint steps.

E_γ (GeV)	p_K (GeV/c)	θ_K (deg)	Lab $d\sigma d\Omega$ (nb/sr)	$\Delta p/p$ (Λ, Σ) (%)	$\Delta p/p$ $(\Sigma, \Lambda\pi)$ (%)	λ (m)	Rate (sec)
1.4	0.674	42.1	646	16.8	20.1	5.1	24.7
2.0	1.041	41.1	203	7.6	6.8	7.8	10.6
2.5	1.321	39.1	88.6	5.3	4.5	9.9	5.0
3.0	1.592	37.1	43.1	4.1	3.4	12.0	2.4
3.4	1.804	35.7	25.8	3.5	2.9	13.6	1.4

Coherent K^+ photoproduction from a complex nucleus will have very small cross sections and we ignore that contribution to target window backgrounds. Quasifree photoproduction will scale roughly as the number of nucleons, modified by Fermi motion and other nuclear corrections. Assuming two 3 *mil* ^{27}Al end windows on a 4 *cm* LH2 target, the relative number of nucleons in the windows is $\approx 4 \times 10^{-2}$, and only some fraction will be kinematically consistent. We therefore neglect any background from unwanted K^+.

Even though various photoproduction cross sections from hydrogen are comparable to each other [26], proton and pion background rates using a bremsstrahlung beam can be large. This is because photon energies well below the endpoint can produce protons and pions with the same momentum as the relatively massive K^+, for a given laboratory angle. We estimate the proton background using the reaction $p(\gamma, p)\pi^0$. The equivalent photon energy is determined by matching the proton angle and momentum to that for the K^+, and the cross section is taken from Ref. [26]. The resulting p/K^+ ratio, including K^+ decay losses is plotted in Fig. 8. It falls from ≈ 250 at $E_\gamma = 1.4\ GeV$ to roughly unity at 3.4 GeV. This is consistent with the DESY experiment [23] ($E_\gamma \approx 1.5\ GeV$) who observed background rates "of the order of 100:1".

We will encounter an additional proton background from *ep* elastic scattering due to the fact that the electron beam passes through the target. Above a certain beam energy, elastic protons enter the SOS acceptance despite the fact that they are systematically higher in momentum than the K^+ and so would be kinematically distinct. Nevertheless, they will contribute to the online trigger rate and we include this process in the p/K^+ ratio plotted in Fig. 8. The contribution rises from zero at 2.0 GeV to $\approx 50:1$ at 3.4 GeV.

We estimate the π^+ background using the reactions $p(\gamma, \pi^+)n, \Delta, \ldots$, following the same procedure as for $p(\gamma, p)\pi^0$. The π^+/K^+ background, also plotted in Fig. 8, falls from $\approx 100:1$ at 1.4 GeV to roughly unity at 3.4 GeV.

Target window contributions to the proton and pion rates were calculated using the

code of O'Connell and Lightbody [32]. There were found to be completely negligible compared to direct proton and pion production on hydrogen.

3.3 Calibrations

Two distinct types of calibration must be considered. The first is the determination of the reconstruction coefficients for the SOS. This is needed for any experiment using this spectrometer, and can presumably be done ahead of time before this proposed experiment consumes specific beam time. The second is monitoring of the acceptance and detectors, including calibrations of the TOF system, which should be done throughout the course of the proposed experiment.

3.3.1 Reconstruction calibrations

The SOS is a "software spectrometer" in that particle trajectories are measured near the focus with arbitrarily placed drift chambers, and we determine the particle's momentum and target parameters using transformation equations in software. These transformation equations are polynomials in x, θ, y, and ϕ near the focus, and the coefficients of those polynomials must be determined.

These reconstruction coefficients can in principle be determined using knowledge (and assumptions) of the magnetic fields and some sort of ray tracing program. However, comparison between the resulting coefficients and those determined empirically using actual data are notoriously inconsistent [33, 34]. Consquently we plan to make use of an empirical calibration using electron scattering under known initial conditions and a "sieve slit" to define the scattering angles [34].

Elastic and near-elastic proton scattering from ^{12}C has been very useful for such calibrations in the LAMPF MRS spectrometer [33], on which the SOS is directly based. One reason for this is that one excites states at 4.4 and 9.6 MeV, as well as the ground state, which provide an excellent way to determine momentum dependence coefficients. We expect to use a similar procedure here. In particular, at a beam energy of 800 MeV and a 35° degree scattering angle, these three cross sections are each quite close to 4 nb/sr [35]. For a 250 mg/cm^2 ^{12}C target ($\Delta E \approx 0.5$ MeV) and a 10μA beam, the luminosity $\mathcal{L}$ is $8 \times 10^{35}/cm^2 sec$. The rate through each sieve slit hole with solid angle ≈ 6 μr [34] would be $\approx 70/hr$. This would be suitable for calibrating, but higher rates could be achieved at lower Q^2 [36], i.e. forward spectrometer angles, although the inelastic cross sections at these specific kinematics are not known.

Table 2: ep Elastic Scattering at $\theta_{LAB} = 39°$

	Detect Electron			Detect Proton		
E	E'	$\Delta E'/E'$	Rate	p_p	$\Delta p/p$	Rate
(GeV)	(GeV)	(%)	$(/sec)$	(GeV/c)	(%)	$(/sec)$
1.4	1.05	±9	1875	1.11	±8	585
2.0	1.36	±11	300	1.38	±9	233
2.5	1.57	±13	83	1.56	±9	135
3.0	1.75	±14	26	1.71	±10	90
3.4	1.88	±15	12	1.82	±10	66

3.3.2 Monitoring using ep Elastic Scattering

At each beam energy for which we take $p(\gamma, K^+)$ data, it will be useful to also calibrate and monitor such things as the spectrometer acceptance and particle detectors. Elastic ep scattering, alternatively detecting either electrons or protons, has been used quite effectively for this purpose [11].

Table 2 lists kinematics and rates for ep elastic scattering into the SOS at 39° and $\mathcal{L} = 10^{37}/cm^2 sec$, i.e. essentially the same conditions as for $p(\gamma, K^+)$ data. We list the detected particle momentum as well as the momentum spread given the ± 60 mr horizontal angular acceptance. There is quite a lot of rate, and a large fraction of the momentum bite is illuminated. Several steps in central momentum could be taken in a short amount of time so that all detectors get a large amount of data for calibration purposes.

4 Experimental Equipment

This experiment will be done with equipment needed for already approved experiments in Hall C. In particular, we will use the SOS as a single arm spectrometer. Particle identification will be carried out using elements from the planned K^+ detector package (Fig. 9) for the SOS, i.e. Time-of-Flight (TOF) hodoscopes and an aerogel Cerenkov counter. Particle identification will be enhanced by (1) moving the first TOF hodoscope to increase the flight path within the detector stack, (2) adding a water Cerenkov counter for online p/K separation at low momenta, and (3) including a layer of shower counter for electron identification during ep elastic calibration. The radiator and (LH2) target can be the same as that for an approved experiment to measure deuteron photodisintegration [37].

This experiment makes no special demands of the SOS. Our maximum incident photon energy is limited only by the maximum central momentum of the SOS, which we have taken

to be 1.8 GeV/c, i.e. $B_{DIPOLE} = 2.0\ T$ and $B_{QUAD} = 1.2\ T$ [30]. Our luminosity is an order of magnitude lower than the calculated maximum [30] for $\theta = 20°$. All calibrations and data taking can be done over an angular range of 35° to 42°, and if need be the spectrometer can be left stationary at 39°.

Particle identification requirements are dictated by proton and pion backgrounds (Fig. 8). π^+ can be distinguished from K^+ with the aerogel Cerenkov counter ($n = 1.03$) over our entire momentum range. To facilitate p/K separation via TOF at the higher momenta, we will move one TOF hodoscope upstream of the first drift chamber. This gains us a longer flight path within the detector stack, and separating the hodoscope layers gives TOF redundancy which reduces non-gaussian tails in the measurement [38]. The only drawback is that the added multiple scattering will limit the momentum resolution. However, K^+ multiple scattering at the *lowest* momentum ($0.67\ GeV/c$) is $< 4\ mr$ for the $1\ cm$ thick scintillator, limiting the momentum resolution to about 0.2%. This is quite satisfactory (Fig. 7).

Additional TOF constraints are applied at the highest momenta by timing relative to the beam pulse [39]. This allows the entire length of the SOS to be used as a flight path, and the p/K time difference at $1.8\ GeV/c$ is $3\ ns$ which is quite sufficient. The nominal beam pulse period will be $2\ ns$. However, it should not be difficult to deliver one pulse every $10\ ns$, for example, keeping a $10\ \mu A$ average current [40]. This removes any possible ambiguities in the start time and makes the TOF analysis trivial.

Kaon identification at lower momenta will be easy offline using TOF, but the total trigger rate will be several kHz due to proton and pion backgrounds. Consequently we would want to reduce the online trigger rate. An index of refraction higher than aerogel is needed to detect K^+ and distinguish them from protons at the lower momenta. However, the index of refraction should not be so high that protons exceed the critical velocity over much of the momentum range. For this reason, we will want to construct and install a Cerenkov counter based on a water ($n = 1.33$) radiator. Such a device would be neither difficult nor costly to provide [41].

Although the planned cryogenic target [37], 10 cm long with $30\ \mu A$ or $\approx 90\ W$ would suffice, this experiment can be done with a 4 cm long, 12 W target.

5 Run Time Request

The actual event rates for both $p(\gamma, K^+)$ (Table 1) and for ep elastic calibrations (Table 2) show that we do not need excessive amounts of running time to collect data. For example $\sim 1\%$ statistics (i.e. $\geq 10^4$ events) can be collected in less than 4 hr even at the lowest event rate ($E_\gamma = 3.4\ GeV$). Our experience [11] with this technique indicates that systematic uncertainties, including spectrometer acceptance and bremsstrahlung calculations, will limit the overall precision to several percent.

Our run time request is based on the following:

- $1.4 \leq E_\gamma \leq 2.5\ GeV$ **in 5 Steps.** 1 hr each for radiator in, radiator out, ep elastic protons, and ep elastic electrons. This is a total of 20 hours.
- $2.5 \leq E_\gamma \leq 3.4\ GeV$ **in 5 Steps.** 4 hr each for radiator in and r adiator out, and 1 hr each for ep elastic protons and ep elastic electrons. This is a total of 50 hours.
- One hour for each energy change, for a total of 10 hours.
- Contingency of 50%

Therefore, our **total run time request is for 7 days, with beam currents up to** 10 μA. This does not include the time needed to determine the spectrometer reconstruction coefficients (Section 3.3.1), or to otherwise commission the SOS.

6 Collaboration Commitments

Our collaboration is composed from a group which carried out a similar experiment in deuteron photodisintegration at SLAC [11], and from groups committed to build the SOS and the detector systems. Specific responsibilities are as follows:

- **CEBAF:** Beamline including position and current monitors, cryogenic target, data acquisition, spectrometer calibrations.
- **BNL:** Drift chambers.
- **Houston:** Aerogel Cerenkov counter.
- **ODU:** TOF and triggering hodoscopes.

In addition, our collaborators from Caltech, Colorado, and Rutgers bring valuable experience both in this photoproduction technique, and with the MRS spectrometer at LAMPF.

7 Future Experiments

We are proposing a specific measurement, namely K^+ photoproduction to $K\Lambda$ and $K\Sigma$ final states at $\theta_{CM} = 90°$ between 1.4 and 3.4 GeV photon energies. However, the physics and the technique lends itself to some natural extensions of this research. These extensions could also be realized quite soon after CEBAF's beam is available.

Angular Distribution of $p(\gamma, K^+)\Lambda$ and $p(\gamma, K^+)\Sigma^0$ reactions. It is possible, using the same instrumentation outlined above, to measure these reactions over some angular range. Some examples are as follows:

- Given the measurements at $\theta_{CM} = 90°$ it is interesting to repeat the procedure at larger angles, again where resonance effects might be important [10]. For example, at $\theta_{CM} = 120°$ the cross section could be measured between 1.6 and 4 GeV with the SOS at an angle of 60°.
- Measurements at 4 GeV by the SLAC group [26] were limited to angles forward of 107° (see Fig. 3), apparently because of decay losses in the 8 GeV spectrometer. Using the technique and equipment described in the proposal, it is straightforward to measure the cross section at $E = 4$ GeV and $100° \leq \theta_{CM} \leq 160°$. It would be necessary to move the SOS to laboratory angles up to 120°.
- At $E_\gamma = 1.4$ GeV there is considerable model sensitivity of the $K\Lambda$ cross section at backward angles [5]. By moving the SOS to a lab angle of 77°, it would be possible to measure the cross section out to $\theta_{CM} = 140°$, where the models differ by a factor of three.

Extension of $\theta_{CM} \leq 90°$ data to higher photon energies. We are limited to $E_\gamma \leq 3.4$ GeV at $\theta_{CM} = 90°$ because of the maximum central momentum of the SOS. Forward angles are restricted to even lower energies. However, the HMS spectrometer observes the same pivot, and its maximum momentum of 6 GeV/c allows photon energies well past CEBAF's maximum energy. The survival fraction is less of a problem as the decay length exceeds 13 m (see Table 1) and the HMS flight path is around 25 m. Particle identification would be accomplished using TOF with the bunched electron beam [26, 28, 39, 40].

Measurement of $p(\gamma, \pi^+)n$ in the 1–4 GeV Region. As with K^+ photoproduction, there is very little data for these intermediate photon energies. For the higher energy data, the s^{-7} dependence of the cross section is clear, while the lower energy data is dominated by resonances [26]. A combination of the SOS and HMS, using the same radiator and target, would make it possible to fill in the data in this region over some range of θ_{CM}. Some of this data may even be taken during the proposed experiment by adjusting the spectrometer momentum and relying on TOF and the aerogel Cerenkov counter to identify pions.

References

[1] R.L.Jaffe and Aneesh Manohar, Nucl.Phys. **B337** (1990) 509

[2] B.R.Holstein, in Proceedings of the 1990 Workshlop on Parity Violation in Electron Scattering, Caltech, E.J.Beise and R.D.McKeown, editors (1990) 27

[3] H.Thom, Phys.Rev. **151** (1966) 1322

[4] F.M.Renard and Y.Renard, Nucl.Phys. **B25** (1971) 490

[5] R.Williams, *et.al.*, Phys.Rev.D **41** (1990) 1449

[6] R.A.Adelseck and B.Saghai, Phys.Rev.C **42** (1990) 108

[7] S.J.Brodsky and G.R.Farrar, Phys.Rev.Lett. **31** (1973) 1153; V.A.Mateev, *et.al.* Lett.Nuov.Cim. **7** (1973) 719; S.J.Brodsky and G.R.Farrar, Phys.Rev. D **11** (1975) 1309; G.P.Lepage and S.J.Brodsky, Phys.Rev. D **22** (1980) 2157

[8] D.Sivers, Ann.Rev.Part.Sci. **32** (1982) 149

[9] Nathan Isgur and C.H.Llewellyn-Smith, Nucl.Phys. **B317** (1989) 526

[10] G.R.Farrar, *et.al.*, Nucl.Phys. **B349** (1991) 655

[11] J.Napolitano, *et.al.*, Phys.Rev.Lett. **61** (1988) 2530; J.Napolitano, *et.al.*, in Proceedings of the 1988 Conference on Intersections between Particle and Nuclear Physics, Rockport, ME, AIP Conference Proceedings 176, G.M.Bunce, editor, (1988) 480; T.Y.Tung, E.R.Kinney, *et.al.*, to be published

[12] R.Schumacher, *et.al.*, CEBAF proposal PR-89-004, "Electromagnetic Production of Hyperons" (1989)

[13] P.L.Dunahoe and R.L.Walker, Phys.Rev. **112** (1958) 981

[14] H.M.Brody, *et.al.*, Phys.Rev. **119** (1960) 1710

[15] R.L.Anderson, *et.al.*, Phys.Rev.Lett. **9** (1962) 131

[16] C.W.Peck, Phys.Rev. **135** (1964) B830

[17] R.L.Anderson, *et.al.*, in Proceedings of the 1965 Lepton Photon Symposium, Hamburg, G. Höhler, *et.al.* editors (1965) 203

[18] S.Mori, Ph.D.Thesis, Cornell University (1966), Unpublished

[19] V.B.Elings, *et.al.*, Phys.Rev. **156** (1967) 1433

[20] D.E.Groom and J.H.Marshall, Phys.Rev. **159** (1967) 1213

[21] A.Bleckmann, *et.al.*, Z.Phys. **239** (1970) 1

[22] T.Fujii, *et.al.*, Phys.Rev.D **2** (1970) 439

[23] H.Göing, *et.al.*, Nucl.Phys. **B26** (1971) 121

[24] D.Decamp, *et.al.*, Orsay Linear Accelerator Report LAL-1236 (1971)

[25] P.Feller, *et.al.*,Nucl.Phys. **B39** (1972) 413

[26] R.L.Anderson, *et.al.*, Phys.Rev.D **14** (1976) 679

[27] Review of Particle Properties, Phys.Lett. **B239** (1990) 1

[28] R.L.Anderson, *et.al.*, Phys.Rev.Lett. **23** (1969) 890

[29] J.L.Matthews and R.O.Owens, Nucl.Instr.Meth. **111** (1973) 157; J.L.Matthews, D.J.S.Findlay, and R.O.Owens, Nucl.Instr.Meth. **180** (1981) 573

[30] See CEBAF Conceptual Design Report, Hall C, April 1990.

[31] R.L.Anderson, Nucl.Instr.Meth. **70** (1969) 87; R.Bell, *et.al.*, SLAC-PUB-557 (1969)

[32] J.W.Lightbody and J.S.O'Connell, Computers in Physics, May/June (1988),57

[33] R.Boudrie, private communication

[34] E.Offerman, *et.al.*, Nucl.Instr.Meth.Phys.Res. **A262** (1987) 298; L.DeVries, *et.al.*, Nucl.Instr.Meth.Phys.Res. **A292** (1990) 629

[35] Hall Crannell, Phys.Rev. **148** (1966) 1107

[36] H.L.Crannell and T.A.Griffy, Phys.Rev. **136** (1964) B1580

[37] R.Holt, *et.al.*, CEBAF proposal PR-89-012, "Two body photodisintegration of the deuteron" (1989)

[38] A.Marini, *et.al.*, Phys.Rev. D **26** (1982) 1777; J.Napolitano, Ph.D. Thesis, Stanford University (1982) Unpublished

[39] R.L.Anderson and D.Porat, Nucl.Instr.Meth. **70** (1969) 77

[40] C.Sinclair, private communication

[41] C.R.Bower, *et.al.*, Nucl.Instr.Meth.Phys.Res. **A252** (1986) 112; A.Bezaguet, *et.al.*, Nucl.Instr.Meth. **158** (1979) 303

Figure Captions

1. Center of mass angles and beam energies of existing and future data points for the reactions $\gamma p \rightarrow K^+\Lambda$ and $\gamma p \rightarrow K^+\Sigma^0$. The solid lines show the region covered by this proposed measurement, with the SOS at a fixed central laboratory angle of 39°. The dotted line shows the approximate region that will be covered by an experiment using the CLAS.

2. Reproduction from Ref. [5] showing Feynman diagrams and resulting fit to data for effective field theory models used to calculate the cross section for $\gamma p \rightarrow K^+\Lambda$.

3. Reproduction of Fig.15 from Ref.[26], showing the consistency of the reactions $\gamma p \rightarrow K^+\Lambda$ and $\gamma p \rightarrow K^+\Sigma^0$ with constituent counting at $E_\gamma = 4$ and 6 GeV. The solid lines are fits to the form $(1-z)^{-5}(1+z)^{-4}$, $z \equiv \cos\theta_{CM}$, which describes data on $\gamma p \rightarrow \pi^+ n$ over a large angular range.

4. Cross section for $\gamma p \rightarrow K^+\Lambda$ plotted as in Fig. 3, but for $E_\gamma = 1.3$ GeV. This is the same data as in Fig. 2. The dashed line is the fit from Fig. 3.

5. Existing data on $K\Lambda$ and $K\Sigma$ photoproduction from hydrogen, for center of mass angles near 90°. The solid lines are model calculations including a fit to the $K\Lambda N$ and $K\Sigma N$ coupling constants [4]. The dashed and dotted lines are obtained by assuming that $d\sigma/dt$ is proportional to s^{-7} [7, 8, 26] and normalizing to the point at 4 GeV (dashed) or to the empirical fit of Fig. 3 (dotted).

6. (a) Schematic of the setup including bremsstrahlung radiator and spectrometer. We can stay quite close to $\theta_{CM} = 90°$ with the spectrometer fixed at a laboratory angle of 39°. However, a few degrees movement around 39° would be best, and should be straightforward to achieve early on. (b) Sample of a spectrum taken at SLAC with the 1.6 GeV spectrometer [28] at fixed beam energy.

7. Final states for $K\Lambda$, $K\Sigma$, and $K\Lambda\pi^0$ are accepted into the SOS simultaneously for photon energies larger than $\approx$ 1.4 GeV. These plots show the thresholds for each reaction, plotted as laboratory momentum versus angle, over the acceptance of the SOS for the lowest and highest photon energies we are considering. The dotted line indicates $\theta_{CM} = 90°$.

8. Estimates of detected proton and pion rates, relative to K^+ rates, in the detector package from electron interactions in hydrogen. The proton rate is dominated by the reaction $p(\gamma,p)\pi^0$ at low energies, whereas at high energies the spectrometer accepts protons from elastic ep scattering. The pion rate is dominated by $p(\gamma,\pi^+)n, \Delta, \ldots$. Particle identification techniques and their effective regions are indicated.

9. Layout of the SOS detector package for this experiment.

FIG.1

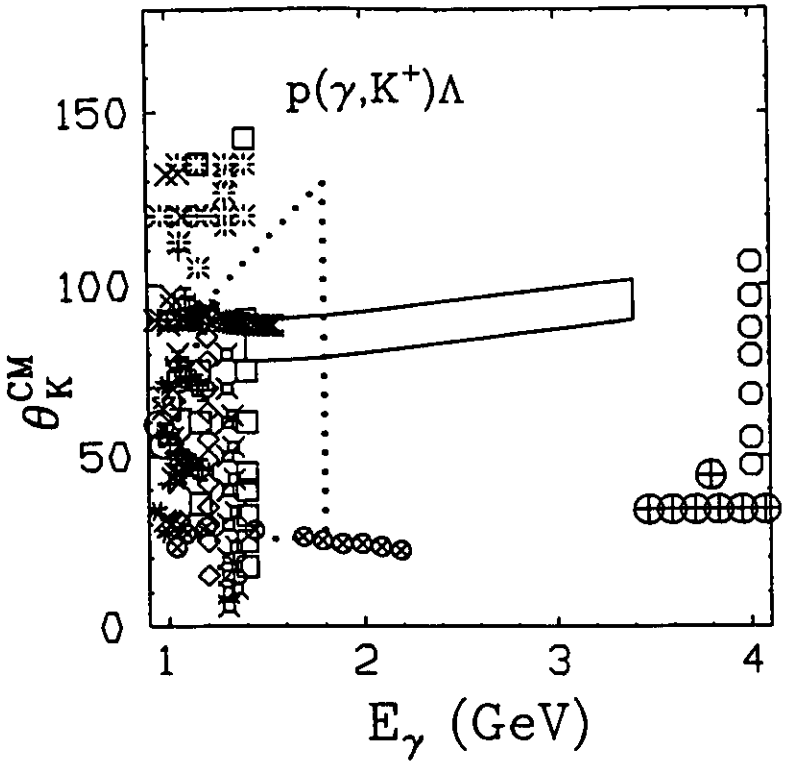

+ CalTech 1958
* CalTech 1960
× Cornell 1962
◇ CalTech 1964
□ Cornell 1965
⊙ Cornell 1966
⊕ MIT 1967
+ CalTech 1967
⋈ Bonn 1970
⊹ Tokyo 1970
⋇ DESY 1971
⁂ Orsay 1971
⊛ Bonn 1972
○ SLAC 1976

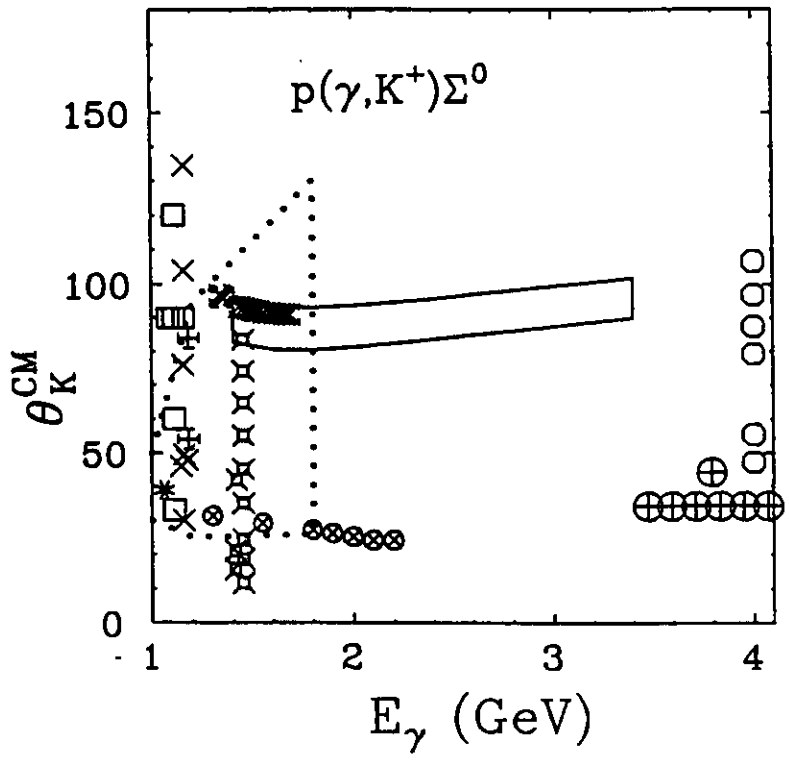

* CalTech 1960
× Cornell 1962
□ Cornell 1965
⊕ MIT 1967
⋈ Bonn 1970
⊹ Tokyo 1970
⋇ DESY 1971
⊛ Bonn 1972
○ SLAC 1976

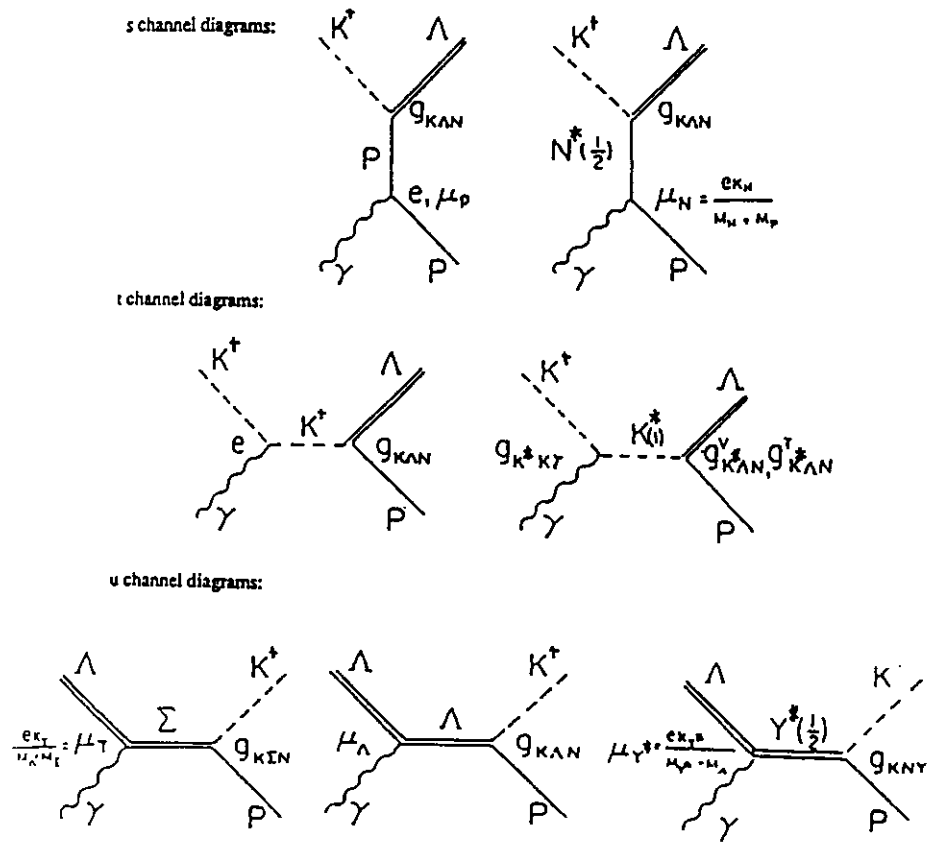

Feynman diagrams for $p(\gamma,K^+)\Lambda$.

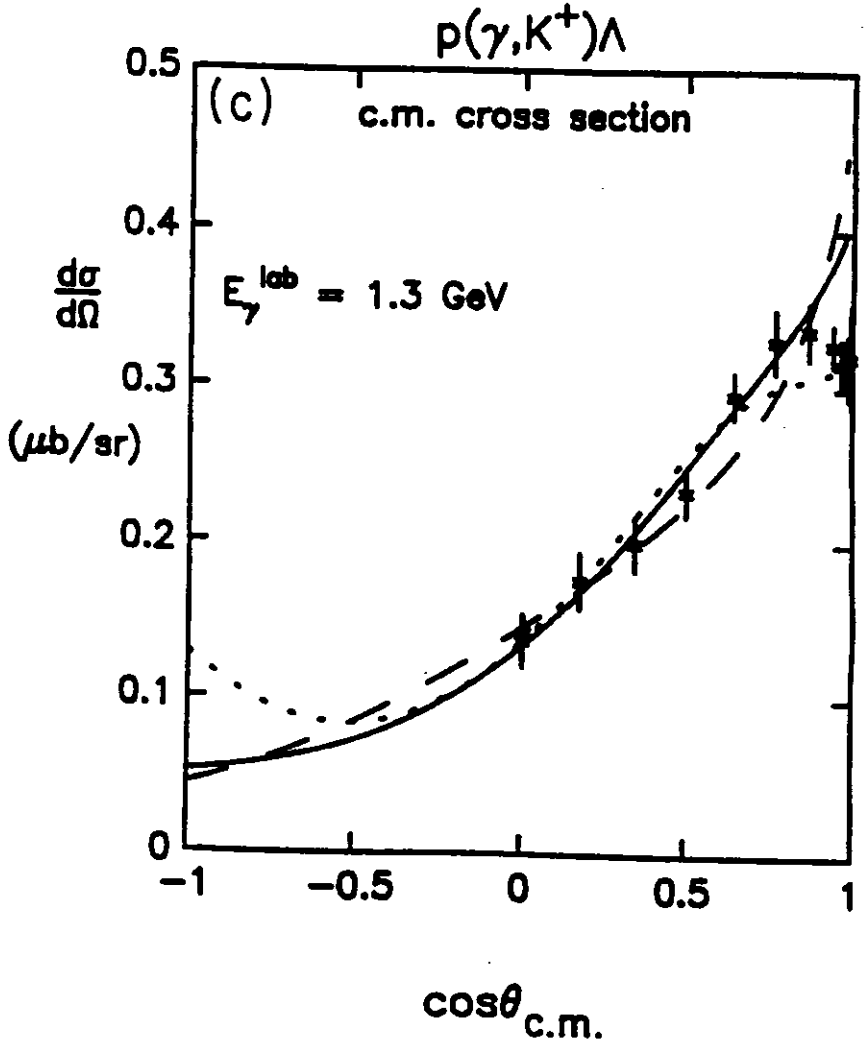

FIG. 2

FIG.3

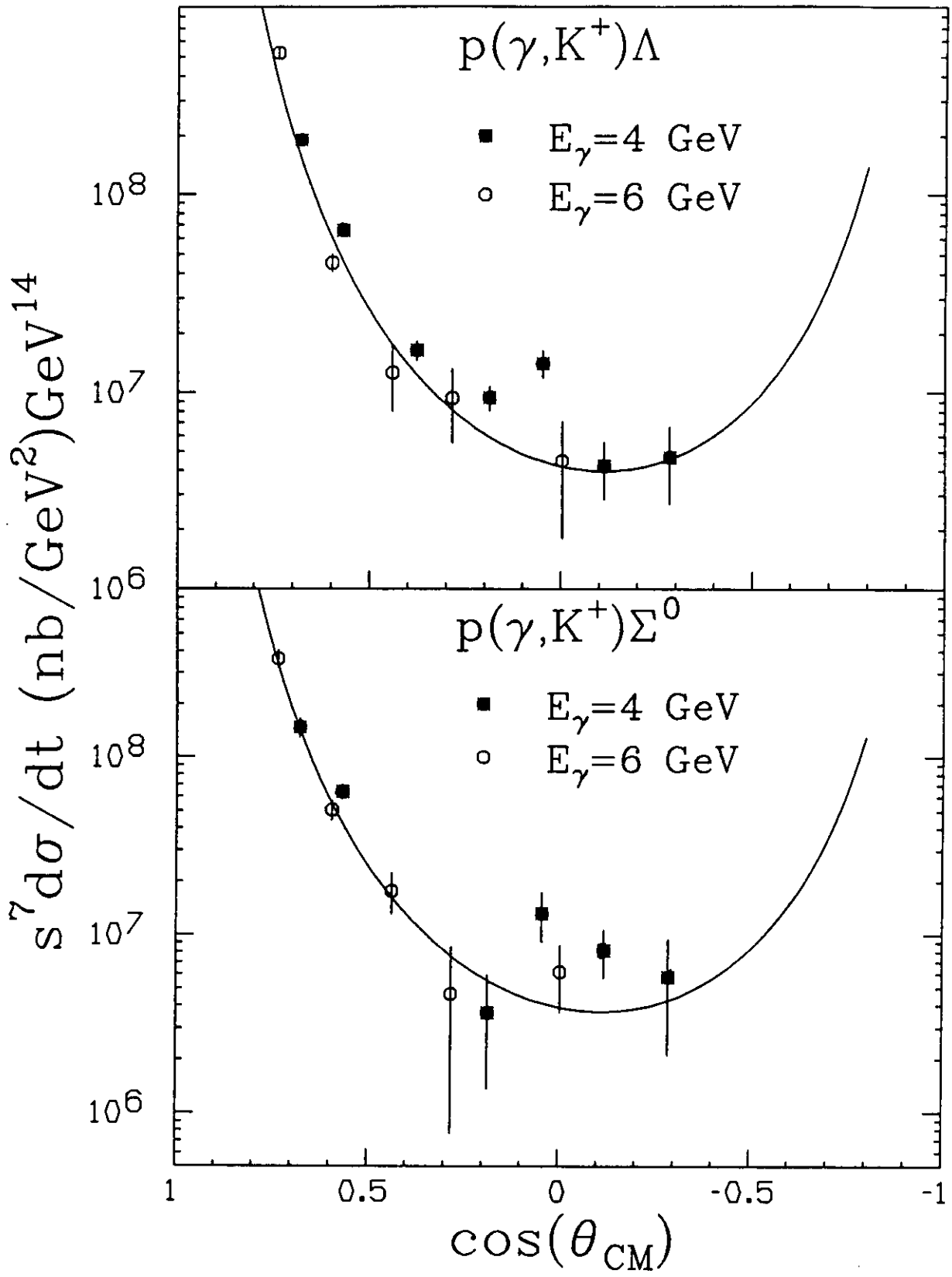
p(γ,K+)Λ
Eγ=4 GeV
Eγ=6 GeV
p(γ,K+)Σ0
Eγ=4 GeV
Eγ=6 GeV
s7dσ/dt (nb/GeV2)GeV14
10^8
10^7
10^6
1
0.5
0
-0.5
-1
cos(θCM)

FIG. 4

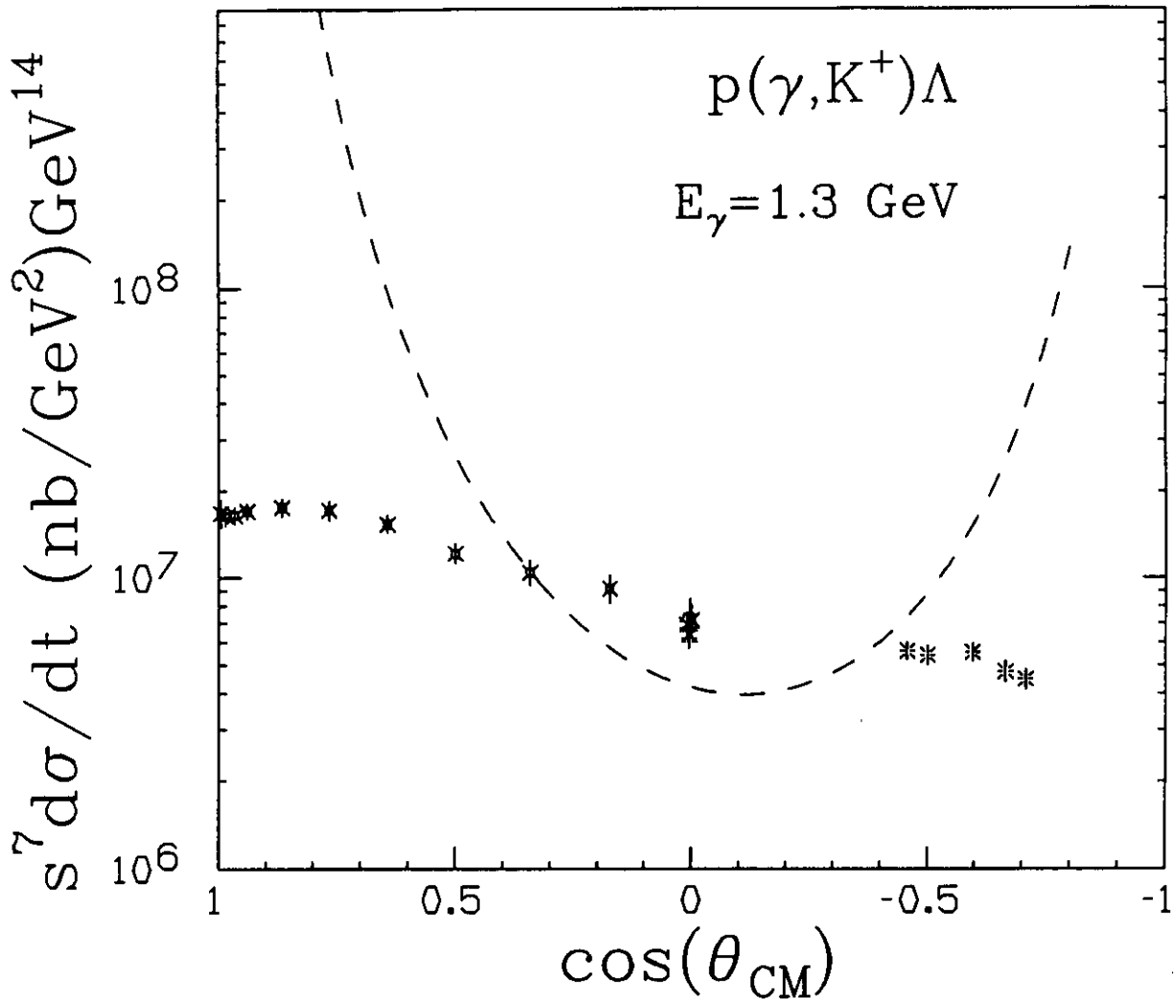

+ CalTech 1967
¤ Bonn 1970
× DESY 1971
⁜ Orsay 1971

FIG. 5

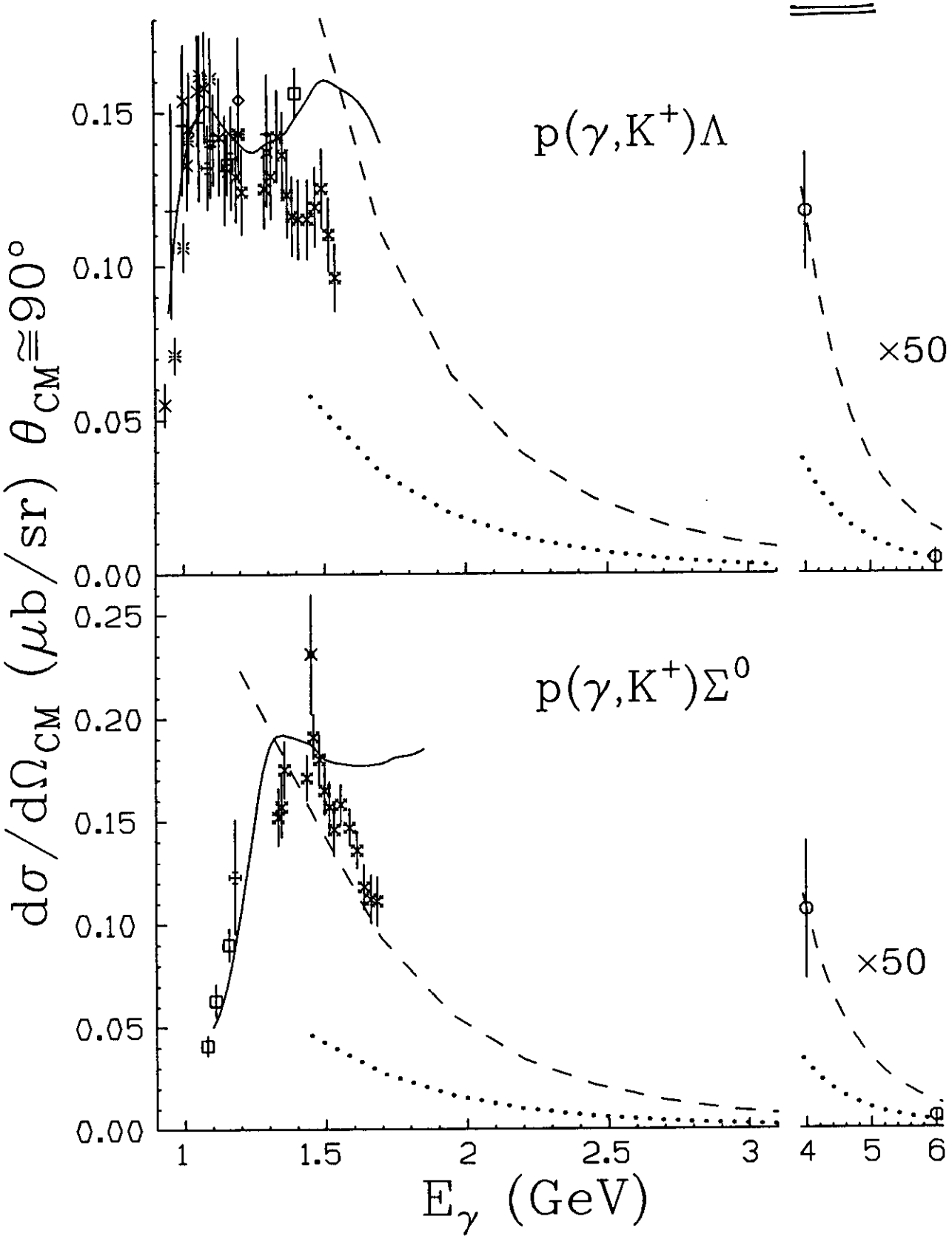
p(γ,K+)Λ
p(γ,K+)Σ0
×50
×50
dσ/dΩCM (μb/sr) θCM≅90°
Eγ (GeV)
0.00
0.05
0.10
0.15
0.20
0.25
1
1.5
2
2.5
3
4
5
6

FIG. 6

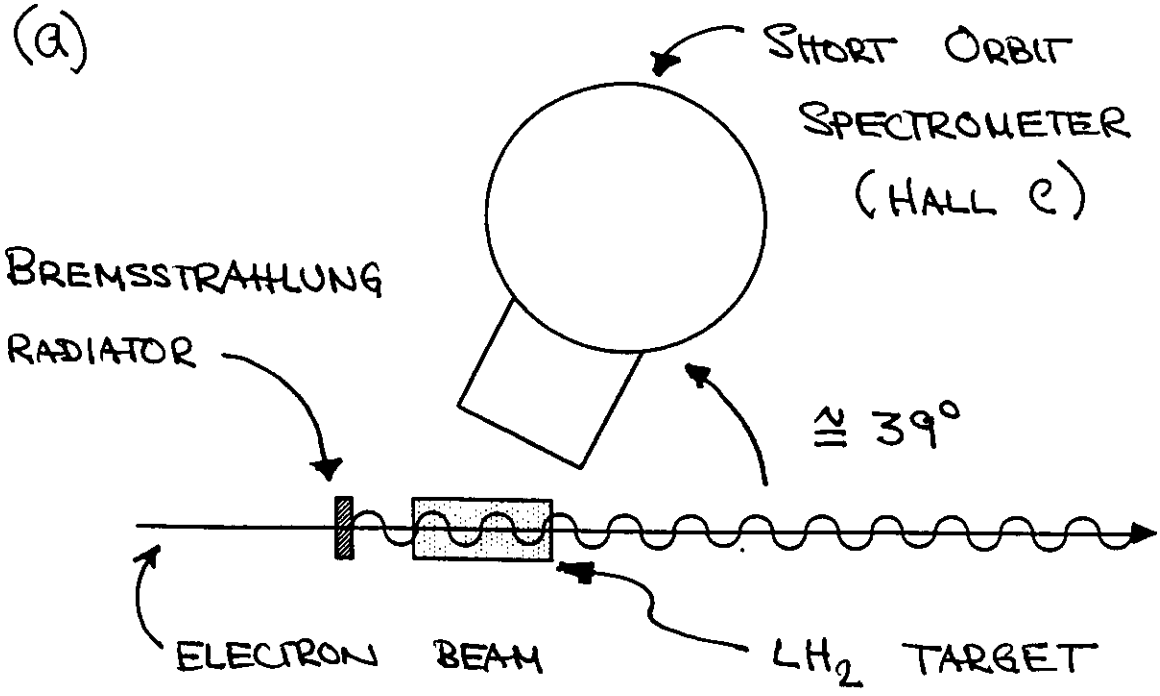
(a)
SHORT ORBIT SPECTROMETER (HALL C)
BREMSSTRAHLUNG RADIATOR
≅ 39°
ELECTRON BEAM
LH2 TARGET

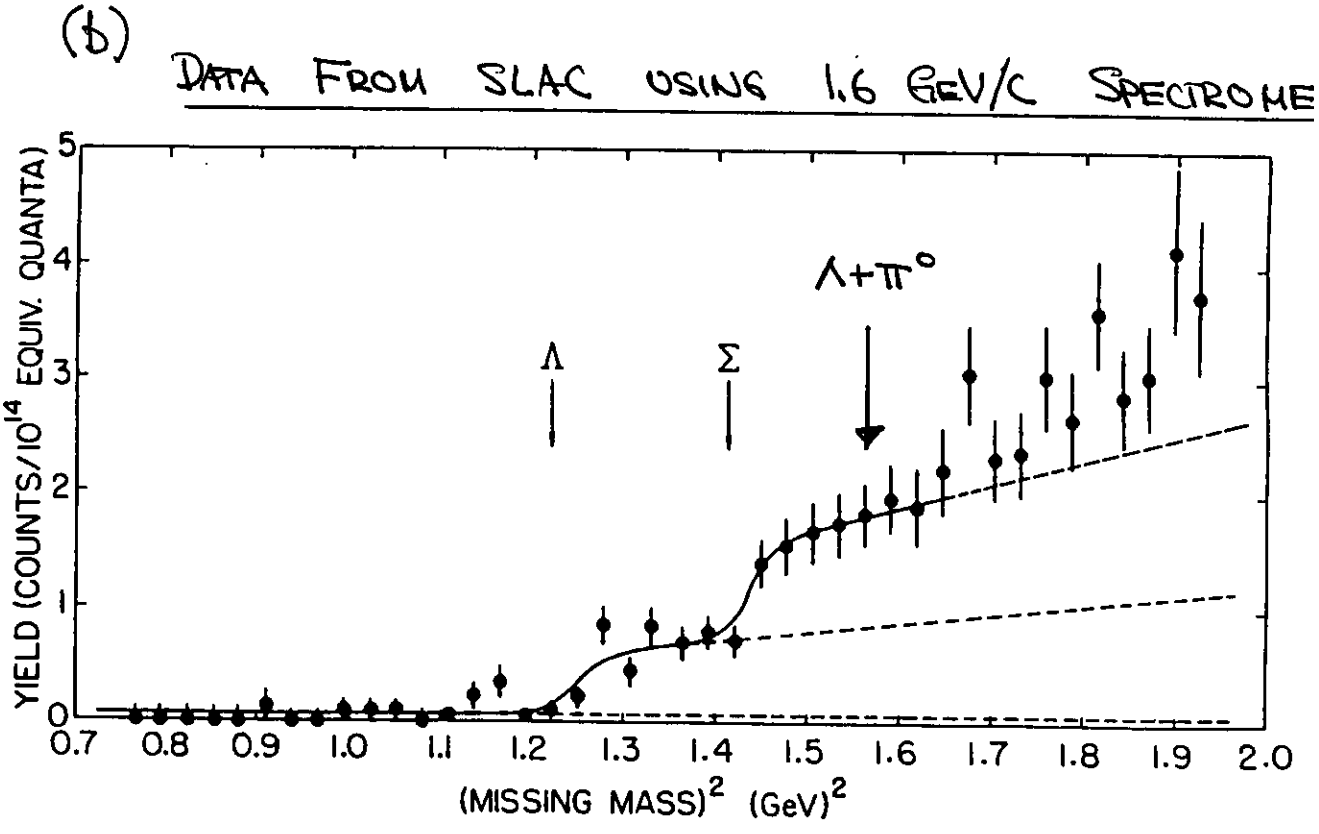
(b)
DATA FROM SLAC USING 1.6 GeV/C SPECTROME
YIELD (COUNTS/10^14 EQUIV. QUANTA)
Λ
Σ
Λ+π°
0
1
2
3
4
5
0.7
0.8
0.9
1.0
1.1
1.2
1.3
1.4
1.5
1.6
1.7
1.8
1.9
2.0
(MISSING MASS)^2 (GeV)^2

FIG. 7

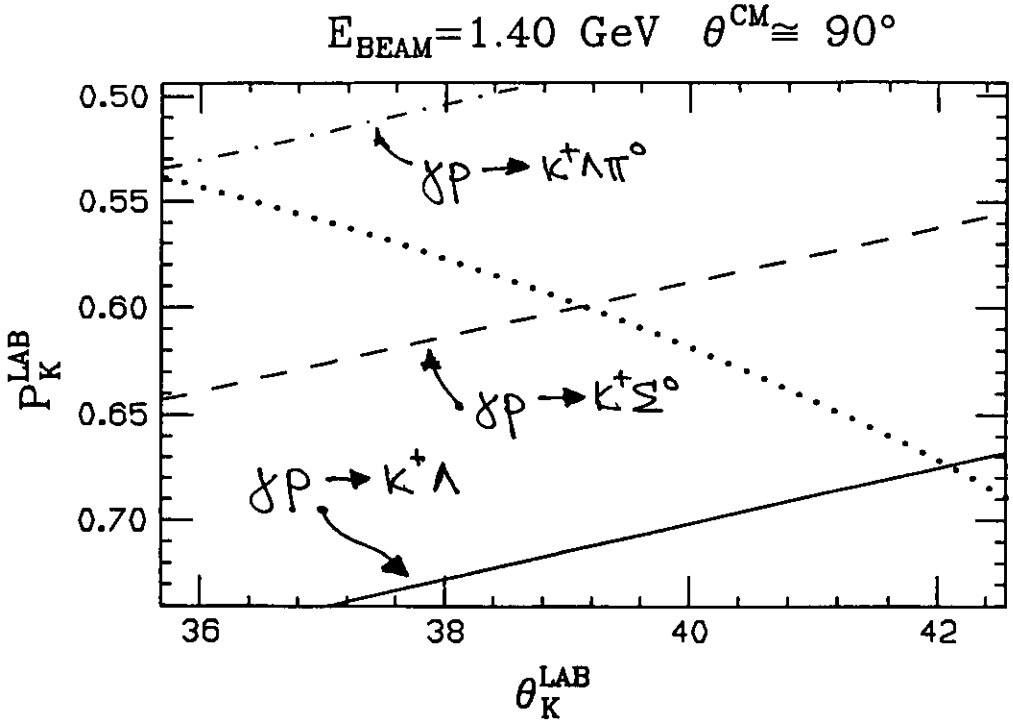
E_{BEAM}=1.40 GeV $\theta^{CM} \cong 90°$
0.50
0.55
0.60
0.65
0.70
P_K^{LAB}
$\gamma p \to K^+ \Lambda \pi^0$
$\gamma p \to K^+ \Sigma^0$
$\gamma p \to K^+ \Lambda$
36
38
40
42
θ_K^{LAB}

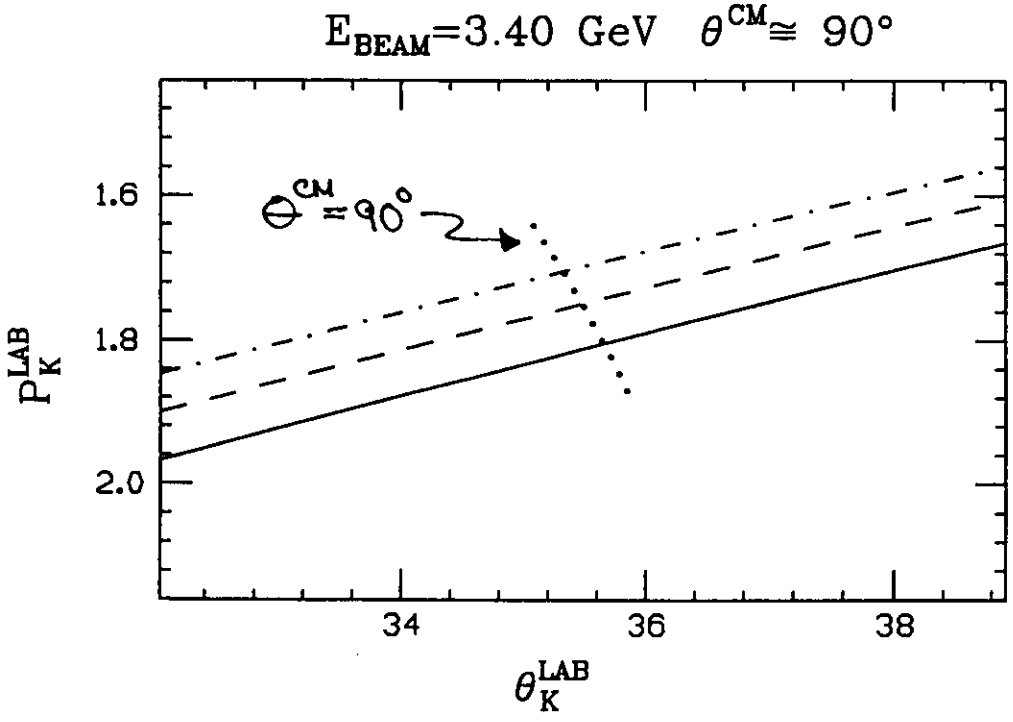
E_{BEAM}=3.40 GeV $\theta^{CM} \cong 90°$
1.6
1.8
2.0
P_K^{LAB}
$\theta^{CM} = 90°$
34
36
38
θ_K^{LAB}

FIG. 8

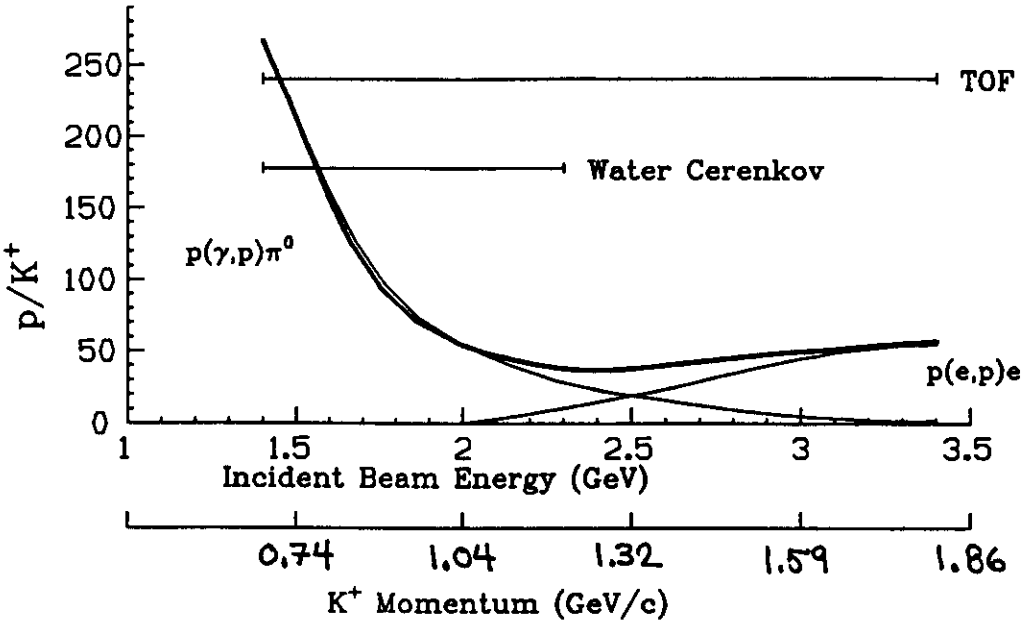
250
200
150
100
50
0
p/K+
TOF
Water Cerenkov
p(γ,p)π0
p(e,p)e
1
1.5
2
2.5
3
3.5
Incident Beam Energy (GeV)
0.74
1.04
1.32
1.59
1.86
K+ Momentum (GeV/c)

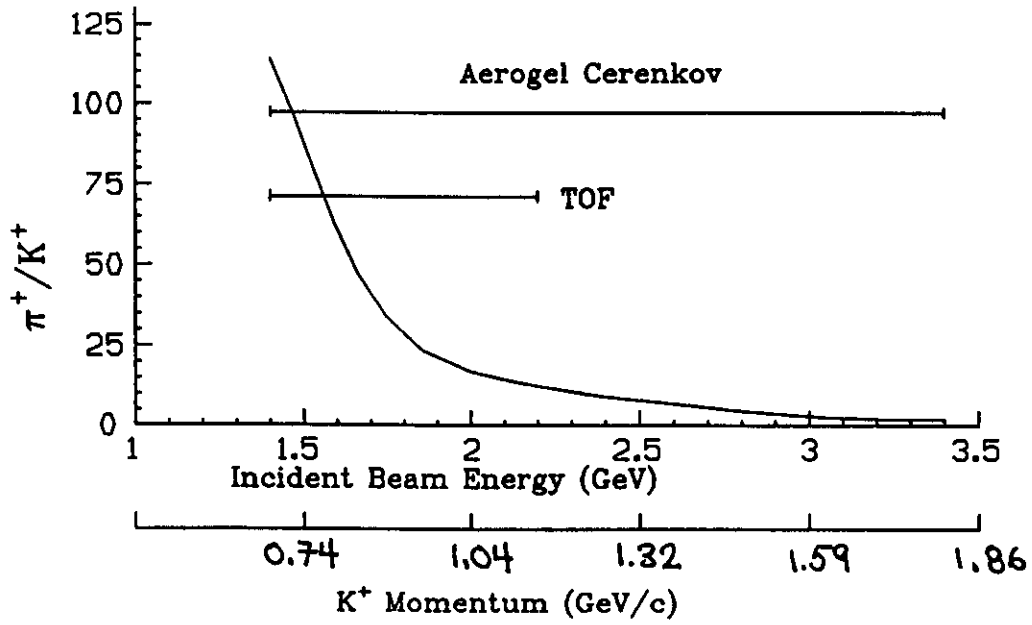
125
100
75
50
25
0
π+/K+
Aerogel Cerenkov
TOF
1
1.5
2
2.5
3
3.5
Incident Beam Energy (GeV)
0.74
1.04
1.32
1.59
1.86
K+ Momentum (GeV/c)

FIG. 9

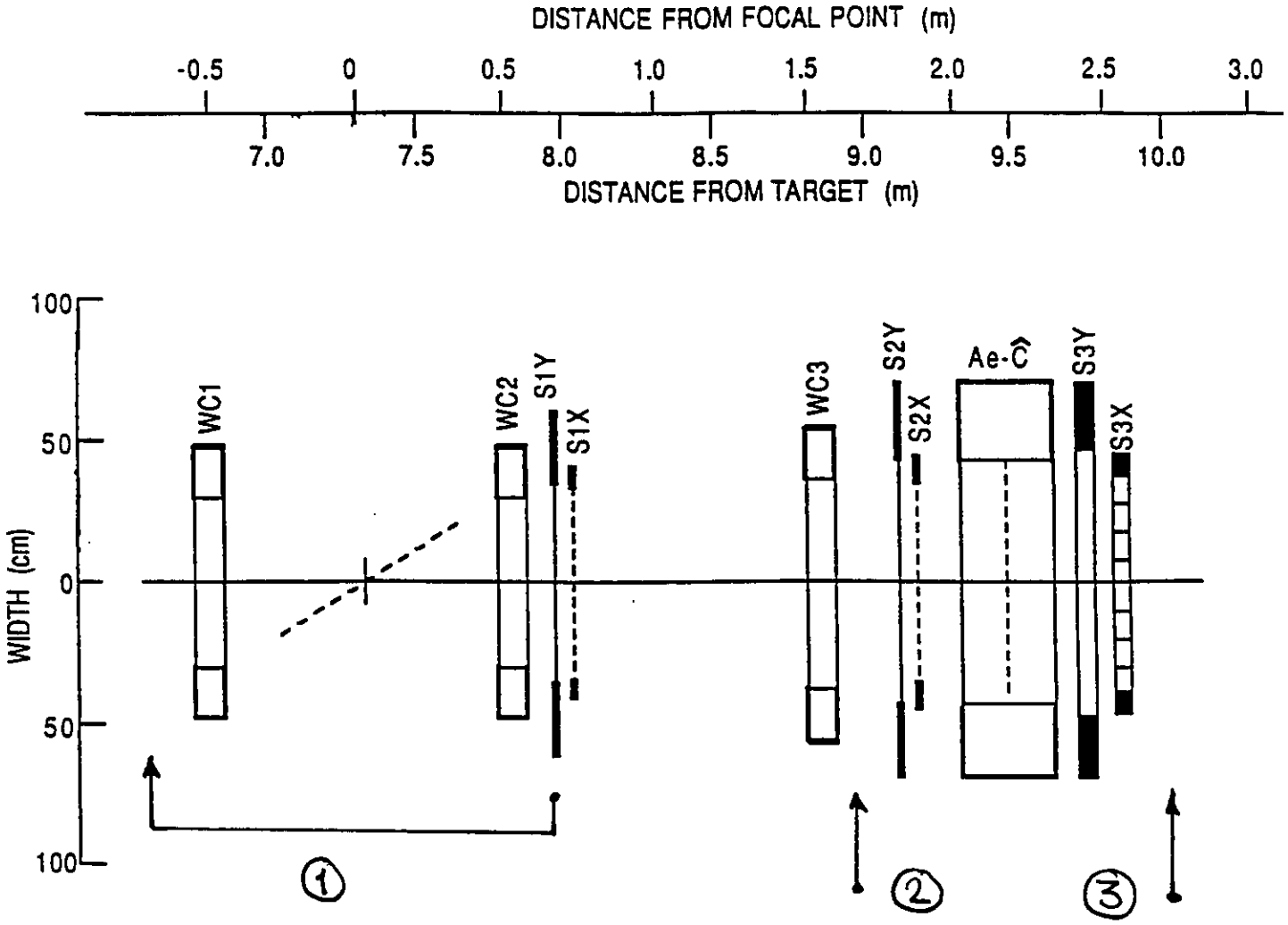

1. MOVE S1y UPSTREAM
2. INSERT WATER ČERENKOV COUNTER
3. INCLUDE SHOWER COUNTER LAYER (FOR ep ELASTIC CALIBRATION)